AAS 15-618

# END OF LIFE DISPOSAL FOR THREE LIBRATION POINT MISSIONS THROUGH MANIPULATION OF THE JACOBI CONSTANT AND ZERO VELOCITY CURVES

**Jeremy D. Petersen[*] and Jonathan M. Brown[†]**

The aim of this investigation is to determine the feasibility of mission disposal by inserting the spacecraft into a heliocentric orbit along the unstable manifold and then manipulating the Jacobi constant to prevent the spacecraft from returning to the Earth-Moon system. This investigation focuses around L1 orbits representative of ACE, WIND, and SOHO. It will model the impulsive ΔV necessary to close the zero velocity curves after escape through the L1 gateway in the circular restricted three body model and also include full ephemeris force models and higher fidelity finite maneuver models for the three spacecraft.

## INTRODUCTION

The Flight Dynamics Facility (FDF) maneuver operations team, located at NASA Goddard Space Flight Center (GSFC), provides the flight dynamics expertise for three Lagrange Point missions: the Advanced Composition Explorer (ACE), the Solar and Heliophysics Observatory (SOHO), and the Global Geospace Science WIND satellite. All three missions are operated by the Space Science Mission Operations (SSMO) Project at GSFC and orbit in the vicinity of the first libration point of the Sun-Earth/Moon system. This region is inherently unstable, so regular stationkeeping is required to maintain their operational orbits at L1. The FDF maneuver operations team provides planning and calibration support for these maneuvers. Each of these missions has been supported for approximately 20 years: ACE launched in 1997, SOHO launched in 1995, and WIND launched in 1994. Given the age of these missions, it is prudent to ensure a proper post-mission disposal strategy has been developed.

The typical mission design process for new missions requires an end-of-mission plan, usually to prevent addition to the ever growing debris environment; however ACE, SOHO, and WIND do not have any documented disposal strategy. It was not yet considered a best-practice during their design and the requirements for libration point missions are vague [NPR 8715.6A]. Other missions and studies have documented various disposal techniques for libration point missions: return to Earth along the unstable manifold[1], disposal into a heliocentric orbit[2], and closing of the zero velocity curves (ZVCs) to prevent Earth return[3].

[*] Systems Engineer, Mission Engineering and Technologies Division, a.i. solutions, Inc., 10001 Derekwood Ln. Ste. 215, Lanham, MD 20706.
[†] Senior Systems Engineer, Mission Engineering and Technologies Division, a.i. solutions, Inc., 10001 Derekwood Ln. Ste. 215, Lanham, MD 20706.

The aim of this investigation is to determine the feasibility of mission disposal by inserting the spacecraft into a heliocentric orbit along the unstable manifold and then manipulating the Jacobi constant and ZVCs to prevent the spacecraft from returning to the Earth-Moon system. Previous work demonstrated that reasonable ranges of impulsive ΔV, on the order of magnitude of tens of m/s, is sufficient to close the ZVCs at the L2 gateway given enough coast time and thus prevent the spacecraft from returning to the Earth-Moon system.[3]

To begin, this investigation will give a brief outline of the three missions, including orbit information and spacecraft properties. The introduction to the three spacecraft will be followed by a brief review of mission disposal requirements and past analysis of disposal for libration point missions. The next section will provide a brief overview of the circular restricted three body problem (CR3BP), including the Jacobi constant and the definition of the ZVCs. With the dynamic model outlined, the focus will move to studying the decommissioning strategy using L1 orbits representative of ACE, SOHO, and WIND operational orbits. It will model the impulsive ΔV necessary to close the ZVCs after escape through the L1 gateway in the CR3BP model. The investigation extends the study to include full ephemeris force models for the three spacecraft to determine the impact of n-body and solar radiation pressure (SRP) modeling over the course of a 200 year propagation.

## MISSION DESCRIPTIONS

Each of the three spacecraft, ACE, WIND, and SOHO, maintain operational orbits at L1, however, each mission operates in a unique Lagrange point orbit (LPO) and contains a unique propulsion system. Despite the difference, all three missions follow the same energy-balancing station keeping strategy. During the maneuver planning process, a maneuver is targeted such that the spacecraft achieves a perpendicular crossing of the rotating libration point (RLP) xz plane after the fourth crossing. Figure 1 shows CR3BP representations for all three missions together on a single plot. The following subsections will provide a brief outline for each spacecraft individually.

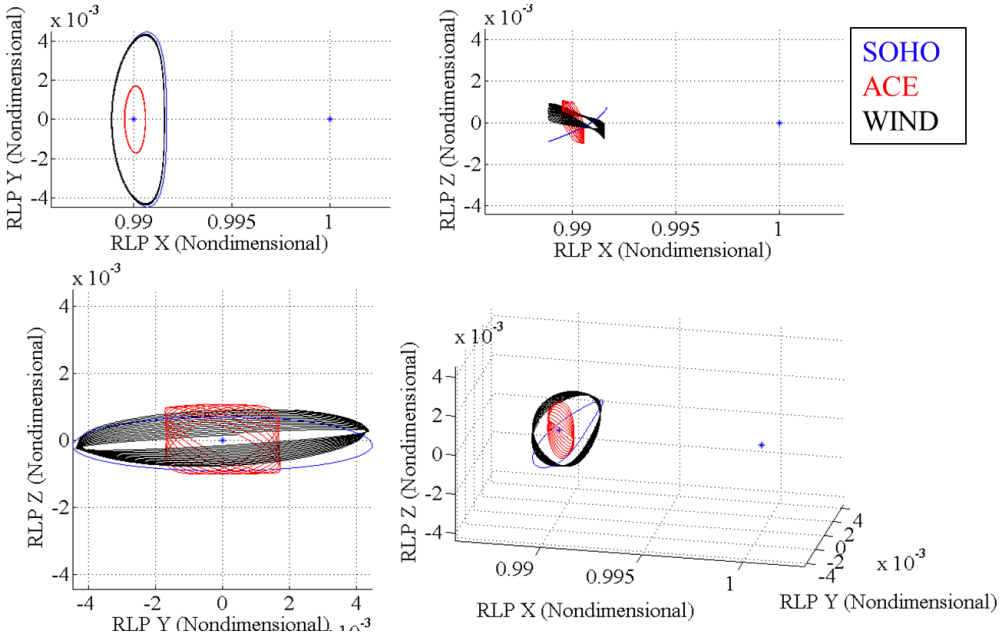


**Figure 1. Planar projections and 3D view of CR3BP representations for ACE, WIND, and SOHO.**

**ACE spacecraft**

The ACE spacecraft, shown in Figure 2, is spin-stabilized with the spin axis (body +Z axis) oriented towards the Sun, completing approximately five rotations per minute. ACE contains a suite of nine science instruments to support the primary science objective of measuring and comparing the composition of several samples of matter, including the solar corona, the solar wind, and other interplanetary particle populations, the local interstellar medium, and galactic matter. The spacecraft is 1.6 meters across and 1 meter high.[4]

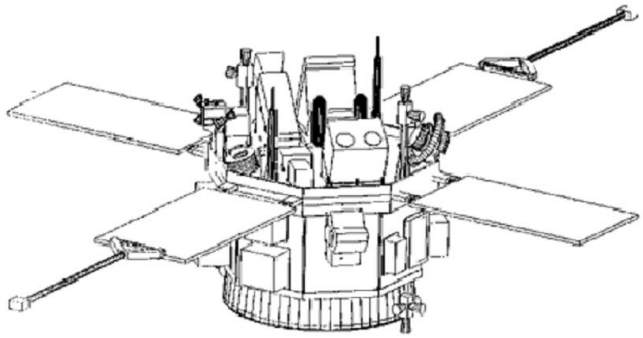

**Figure 2. The Advanced Composition Explorer (ACE) Spacecraft[4]**

The spacecraft propulsion system is a blow-down monopropellant hydrazine system with four conispherical fuel tanks and carries 10 thrusters rated at nominal 1-lbf thrust and 228-second specific impulse. Four thrusters are mounted in an axial configuration, two on the top deck facing the sun and two on the bottom deck facing toward the Earth. These four thrusters provide $\Delta V$ control parallel to the spin axis. The remaining six thrusters are mounted radially and provide velocity control within the spin plane, spin-axis reorientation, or spin rate control depending on the combination of thrusters used. All four tanks are connected such that all thrusters draw from the entire system simultaneously, however because the four tanks were not filled equally, two tanks are currently empty and have been isolated from the system by closing their latch valves. This has only a minor impact on the propulsion system performance, and the blow-down curve for the remaining two tanks is slightly steeper.

The ACE spacecraft operates in a small-amplitude Lissajous orbit about the Sun-Earth/Moon L1 libration point. As seen from the Earth, the ACE Lissajous orbit has approximate nominal amplitudes centered on L1 of 6 degrees out-of-plane and 10 degrees in-plane. In three-dimensional Cartesian terms using the RLP reference frame, the x-amplitude is approximately 80,000 km, the y-amplitude is approximately 260,000 km, and the z-amplitude is approximately 158,000 km.

Because the spin axis is oriented roughly along the Earth-Sun line, any changes in the energy of the orbit are applied using the axial thrusters. These maneuvers are commanded with a constant firing time, which applies the entire maneuver in a single burn segment.

**SOHO Spacecraft**

The SOHO spacecraft, shown in Figure 3, is a three-axis stabilized spacecraft that maintains one axis (body +X axis) fixed upon the Sun's center at all times. It carries a suite of 12 instruments to study phenomena relating to the solar surface and atmosphere, solar dynamics, and the solar corona and solar wind. The propulsion system is comprised of a blow-down monopropellant hydrazine system containing 2 sets of 8 thrusters (primary and redundant set), each with a specific

impulse of 220 seconds and a thrust rating of 4.2 Newtons at beginning of life and 2.2 Newtons end of life.

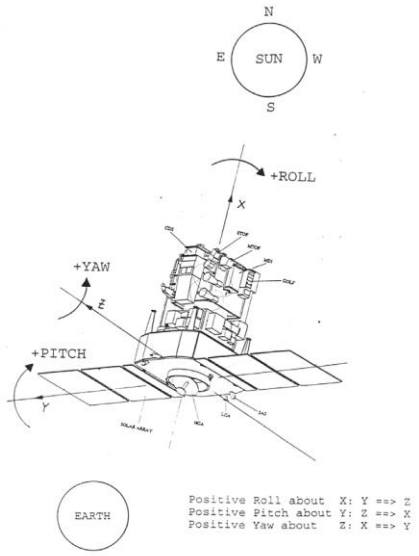


**Figure 3. The Solar and Heliospheric Observatory (SOHO) Spacecraft[5]**

The SOHO spacecraft operates in a quasi-halo orbit about the Sun-Earth/Moon L1 libration point. During the pre-launch design phase, the minimum allowable Sun-Earth-Vehicle (SEV) angle can was specified 4.5 degrees and the maximum allowable angle is 32 degrees. Taking these considerations into account, the final orbit selected resulted in a minimum SEV angle close to 4.5 degrees when the spacecraft crosses the RLP xz plane on the Earth-side of L1. At the extreme y-axis locations along that orbit, the SEV angle is never more than 25.5 degrees. This results in an orbit with x-amplitude of 206,000 km, y-amplitude of 667,000 km, and z-amplitude of 120,000 km.

A series of anomalies in the late 1990s nearly resulted in the loss of the mission and required permanent modifications to the maneuver execution procedure.[5] All three of SOHO's gyroscopes failed and required a complete rewrite of the spacecraft onboard attitude control system. The original maneuver strategy relied on the gyroscopes as part of the closed-loop control mode to provide attitude control during the maneuver. With the gyroscopes no longer functioning, the pulse sequences for each thruster are computed to minimize wheel torques and preserve attitude stability during the burn. As a consequence, the two main thrusters are limited to an average duty cycle of 5%, and either one or two additional thrusters are fired at about 0.1% duty cycle to help control the attitude.[2] In between maneuver pulses, the star trackers compute the attitude and rates, and the reaction wheels correct the error before the next thruster pulse. Because the thruster duty cycles are only 5%, the overall maneuver duration will typically exceed 1000 seconds even for relatively small maneuver magnitudes (less than 50 cm/s).

### WIND Spacecraft

The WIND spacecraft is spin-stabilized with the spin axis (body +z axis) oriented towards the south ecliptic pole (SEP), completing approximately 20 rotations per minute. The spacecraft has a cylindrical body, approximately 1.8 meters in height with a diameter of 2.4 meters. As shown in Figure 4, a series of booms and wires extend outward both radially and axially from the main body with sensors for some of the eight science instruments onboard. The primary science objec-

tives of the WIND mission are proving complete plasma, energetic particle and magnetic field for magnetospheric and ionospheric studies, investigate basic plasma processes occurring in the near-Earth solar wind, and provide baseline, 1 AU, ecliptic plane observations for inner and outer heliospheric missions. The spacecraft contains two sets of four 22 Newton hydrazine thrusters and one set of four 2.2 Newton thrusters. With the spin axis oriented towards the SEP, the radial thrusters are used for LPO stationkeeping maneuvers to provide $\Delta V$ in the ecliptic plane. The axial thrusters provide $\Delta V$ normal to the ecliptic plane.[6]

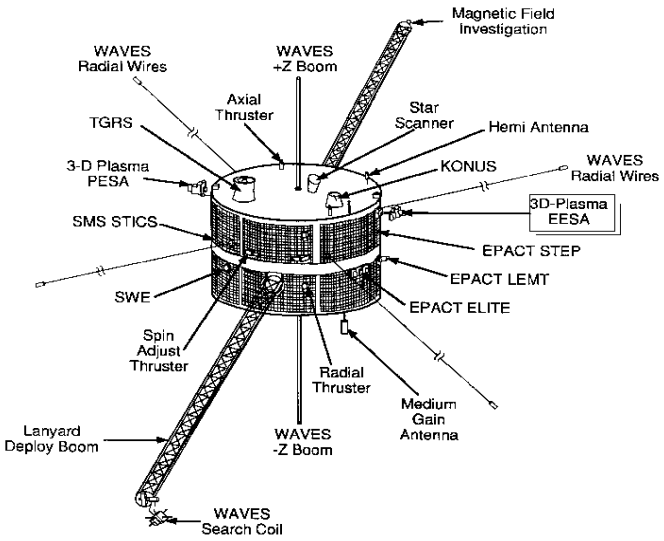


**Figure 4. The WIND Spacecraft and Instruments.[6]**

After launching in 1994, WIND spent a decade traversing the Earth-Moon system. The trajectory during this time included several double lunar swingbys to control the line of apsides, lunar backflip transfers in order to reorient the line of apsides, a series of distant prograde orbits, and 38 targeted lunar flybys. Following the final lunar flyby in late 2002, WIND was sent on a single loop around L1 and then briefly returned to the Earth-Moon system before being flung out to L2. The spacecraft again completed a single loop around the libration point, fell back into the Earth-Moon system, and was flung back to L1 where it arrived in mid-2004. The spacecraft was inserted into a large amplitude Lissajous orbit with dimensions slightly smaller than SOHO's halo orbit and has remained there for the over a decade.[7,8,9,10]

WIND has a unique maneuver execution strategy due to the orientation of the spin axis towards the SEP. Instead of performing a continuous burn, like ACE, WIND performs an integer number of identical pulses using the radial thrusters. A maneuver plan is composed of three elements: the number of pulses, the pulse width, and the jet start angle. The number of pulses indicates how many identical pulses are required to achieve the desired $\Delta V$. The pulse width, measured in the spin plane, denotes the angle of rotation through which each thruster should fire per pulse. The jet start angle, also measured in the spin plane, is the angle where the pulse begins and is measured relative to the point where the sun sensor detects the Sun. The pulse width and jet start angles are different for each thruster, and they are computed such that the minimum perturbation is applied to the spin rate and spin axis orientation.

## END OF LIFE DISPOSAL

WIND, SOHO, and ACE are all operating nominally with sufficient propellant to remain at L1 for years to decades, and they continue to return valuable scientific measurements from their outposts roughly 1.5 million km from Earth. However, the spacecraft were launch 21, 20, and 18 years ago, respectively. Realistically speaking, they are approaching the end of their operational lifetimes. There were no definitive plans for their decommissioning created prior to launch, so to determine a strategy for these missions we first examine existing policies and procedures, as well as historical precedents set by other missions.

### NASA Procedural Requirements

NASA has established requirements for end-of-mission planning which include standards for limiting debris in the orbit regimes that are most densely-populated with active missions [NPR 8715.6A]. Spacecraft must be removed from these protected regions within 25 years after the mission is completed; or, if the mission lasts longer than five years, the spacecraft must be removed 30 years after launch. For low Earth orbits this is most frequently accomplished by lowering the orbit, either actively with thrusters or passively due to atmospheric drag, and re-entering the atmosphere. Because re-entry is not practical for many satellites in the upper reaches of low earth orbit, or for nearly any mission in medium or geosynchronous Earth orbits, several altitude bands have been defined for graveyard orbits. These regions are essentially unused for active missions, so defunct missions can be safely decommissioned here with less propellant expense than atmospheric re-entry would require.

Interplanetary missions, including heliocentric trajectories, have a distinct set of requirements to fulfill both during operations and after decommissioning [NPR 8020.12D], with the primary goal of preventing inadvertent biological contamination. However, for deep space missions that do not target a planetary body, such as libration point orbiters, none of these requirements are imposed unless an Earth return is planned (e.g. Genesis).

### Past Mission Examples and Decommissioning Options

The lack of requirements may in part be a result of so few missions operating in these exempt orbit regimes. There have been only 11 missions sent to L1 and/or L2 in the Sun-Earth/Moon system, five of which are currently active and maintaining their science orbits. Of the six spacecraft to depart the libration point region at the end of their missions, three were sent toward new targets: ISEE-3 was sent to make the first-ever flyby of a comet, Genesis was a sample-return mission and re-entered Earth's atmosphere, and Chang'e 2 visited an asteroid. This leaves three missions which decommissioned directly from L2: WMAP, Herschel, and Planck. All were placed into heliocentric orbits outside of Earth's orbit.

In addition to the examples set by past missions, several studies of possible decommissioning techniques have been completed. The most common strategies are controlled Earth re-entry, lunar impact, and heliocentric orbit. The Earth re-entry and lunar impact options are similar in that they fully eliminate the risks of uncontrolled Earth re-entry as well as conjunctions with other spacecraft after completion. Lunar impact also has the potential benefit for additional science to be collected, though it is unclear of the scientific community would be interested. However, both options require precise navigation in order to achieve their targets, and any sufficiently large errors could increase risk to people on the ground and/or other spacecraft.

Heliocentric orbit disposal is accomplished by performing a maneuver to depart the libration point region along the unstable manifold that results in a heliocentric orbit rather than returning to the Earth's gravity well. In selecting the maneuver timing and magnitude, a long duration simulation can be performed to ensure the satellite does not return to Earth within some desired time

period. A more robust method of maneuver design is accomplished by analyzing the dynamics of the CR3BP. The maneuver can be designed to increase the Jacobi Constant such that the ZVCs are closed at the gateway near the libration point. Once the ZVCs have been closed, the spacecraft is then prevented from ever returning to the vicinity of the Earth. This ΔV will likely be on the order of hundreds of meters per second, but it is possible to reduce the magnitude by performing a small initial maneuver to perturb the spacecraft off its operational orbit and then performing a larger second burn to close the ZVCs when the spacecraft is farther from the Earth. The downside to this approach is that operations must continue for multiple months until the final maneuver is performed, which extends operational costs.

Though Earth re-entry and lunar impact are interesting problems in terms of navigation and maneuver design, heliocentric disposal is much simpler with fewer risks. Though SSMO has not yet selected a disposal method for ACE, SOHO, or WIND, this analysis will focus on the heliocentric disposal option using multiple maneuvers in order to reduce the total fuel required.

## ANALYTICAL CIRCULAR RESTRICTED THREE BODY PROBLEM

The CR3BP model is an ideal tool for studying LPOs. As a background, the CR3BP models the motion of two larger primaries (Sun and Earth/Moon barycenter for this application) that are assumed to move in circular orbits about their mutual center of mass. A third, massless body is fixed in a rotating reference frame such that the x-axis is the line from the larger to the smaller primary, the z-axis is normal to the plane of motion along the angular momentum vector of the rotating primaries, and the y-axis completes the right-handed triad. Figure 5 shows a visual representation of the CR3BP. The nondimensional equations of motion are captured in equation 1. For this analysis a characteristic length, representative of the mean Sun-Earth distance, of 149,587,457 km is used to nondimensionalize the system. This corresponds to a characteristic time of 5,022,110 seconds.

$$\ddot{x} - 2\dot{y} = \frac{\partial U^*}{\partial x} \quad \ddot{y} + 2\dot{x} = \frac{\partial U^*}{\partial y} \quad \ddot{z} = \frac{\partial U^*}{\partial z}$$

$$U^* = \frac{1-\mu}{d} + \frac{\mu}{r} + \frac{1}{2}(x^2+y^2) \tag{1}$$

$$d = \sqrt{(x+\mu)^2 + y^2+z^2} \quad r = \sqrt{(x-1+\mu)^2 + y^2+z^2}$$

One of the primary features of the CR3BP model is that the equations of motion contain an integral of motion, the Jacobi constant. The Jacobi constant is an energy-like quantity that provides useful information about the properties of a given state. The equation associated with the Jacobi constant is shown in equation 2. The constant is simply a function of the state of the spacecraft and the mass ratio between the two primaries. An important feature of the Jacobi constant is the existence of a zero velocity surface that controls the boundaries of the spacecraft's trajectory. Studying equation 2, if the velocity component is set to zero and the Jacobi constant, C, is fixed at a given energy, the position coordinates create a boundary curve called the zero velocity curves (ZVCs).

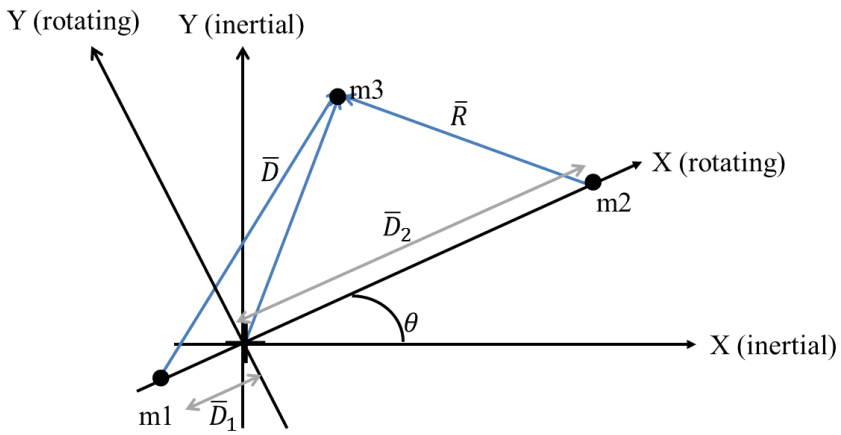


**Figure 5. Diagram outlining the CR3BP system. For this investigation, m1 is the sun and m2 is the Earth/Moon barycenter.**

$$C = 2U - V^2 \tag{2}$$

The evolution of the ZVCs follows a specific pattern as the Jacobi constant changes, shown in Figure 6. At first, the ZVCs are two independent circles. In this state, the spacecraft is bound to one of the two primaries. It cannot travel to the other primary, as shown by the gray region, called the exclusion zone, in between the two primaries. The gray region corresponds to those position coordinates at a specific Jacobi constant resulting in a physically impossible negative velocity term. As the Jacobi constant decreases, the two independent circles begin to expand and converge at L1. Once this energy level is reached, travel between the two primaries becomes possible. This event is described as opening the L1 gateway. Continuing the evolution of the ZVCs, the next event is the opening of the L2 gateway. At this point, travel outside of the ZVCs becomes permissible. Eventually, the pattern continues and the L3 gateway opens. Finally, the ZVCs converge on L4 and L5 and eventually disappear altogether. At this state, travel anywhere in the xy plane portion of system is possible.

Mission designers can use the evolution of the ZVCs to their advantage when planning for end-of-life disposal. Figure 7 shows the ZVCs for a sample halo orbit that mimics SOHO's operational orbit in blue. As seen in the blue lines, the ZVCs are open at L1. At this energy level, the spacecraft can travel freely back to Earth or towards the Sun. Ideally, a spacecraft disposal strategy aims to limit the possibility for return to the operational orbit it inhabited. As discussed above, the ZVCs provide a physical boundary that a spacecraft cannot cross in this CR3BP approximation. Closing the L1 gateway, as shown by the black curve in Figure 7, while the spacecraft is on the Sun side of L1 would prevent it from returning to the Earth-Moon system.

The primary concern for closing the L1 gateway is the ΔV cost associated with changing the Jacobi constant. Previous work demonstrated that reasonable ΔV costs (tens of m/s) can be achieved for an L2 gateway closing maneuver given a proper time of flight after a departure maneuver from the operational orbit.[3] The previous study investigated ΔV costs around the L2 gateway. For application involving ACE, WIND, and SOHO, the investigation will focus on the ΔV costs associated with closing L1 gateway.

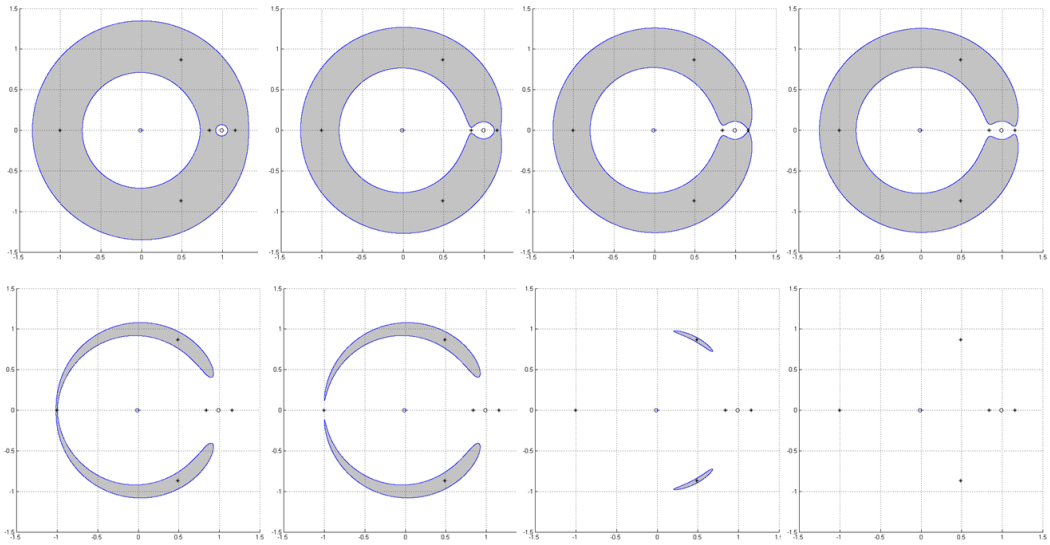

**Figure 6. Evolution of the ZVCs as the Jacobi constant decrease. The blue lines are the ZVCs, the grey region is the exclusion zone, and the stars represent the sun, earth, and five Lagrange points of the CR3BP.**

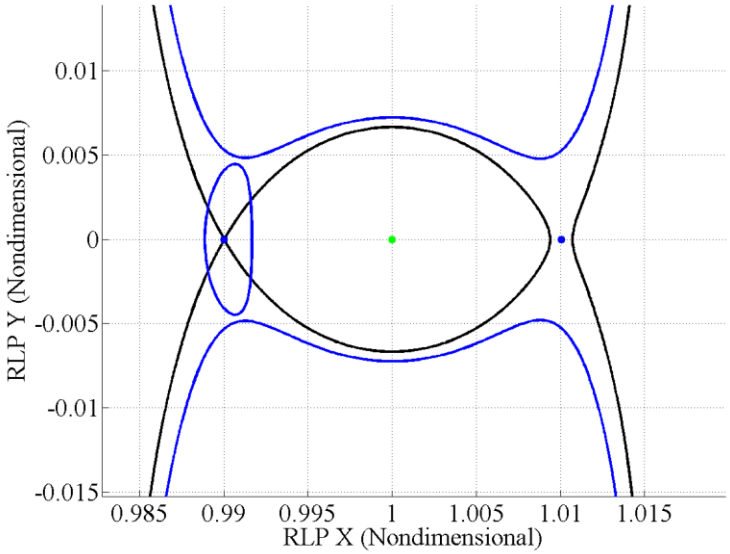


**Figure 7. Planar projection of SOHO's orbit along with the corresponding ZVCs. The blue ZVCs match the energy of SOHO's orbit (also in blue). The black lines show the ZVCs corresponding to the energy level at L1. The black ZVCs represent a closed L1 gateway.**

Using SOHO as an example, a baseline halo orbit representative of the operational orbit was generated within the CR3BP model. This orbit can be seen in Figure 1. Once the baseline orbit is established, the orbit is discretized and a departure $\Delta V$ is applied at each discretized point. Along each departure arc, the $\Delta V$ required to change the Jacobi constant to a level such that the L1 gateway is closed is calculated. This calculation, shown in equation 3, is done using a simple algebraic manipulation of the Jacobi integral. The current state of the spacecraft is known, along

with the desired Jacobi constant required to close the L1 gateway and therefore the ΔV required to change the Jacobi constant from the current state value to the desired value can be calculated.[3] The resulting ΔV is applied along the anti-velocity direction as the goal is to remove energy from the system such that the L1 gateway closes. Figure 9 shows the resulting departure arcs propagated for approximately 400 days. The color scheme, shown in Figure 8, visualizes different departure locations along the reference halo orbit, based on a defined departure phase. The departure phase is an angle measured in the ecliptic plane relative to the RLP-X axis, with zero starting on the Earth facing side of L1 along the RLP-X axis, and increases counterclockwise along the baseline orbit. Figure 10 demonstrates the ΔV cost along an entire trajectory arc (single color arc from Figure 9) as a function of time past the departure maneuver. The ΔV range is quite large with some ΔV requiring over 200 m/s. The blank regions in Figure 10 corresponds to locations along the departure arc in which the spacecraft is located within the negative velocity regions of the ZVCs associated with a closed L1 gateway. Given a long enough time of flight, the maneuver size begins to decrease to reasonable values under 15 m/s.

$$\Delta V = |\bar{V}| - \sqrt{2U - C_{Target}} \tag{3}$$

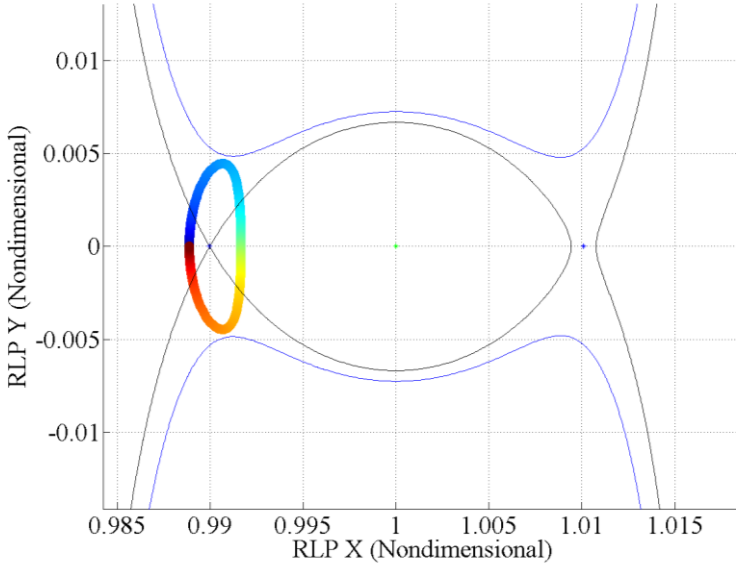


**Figure 8. Example of the color scheme used to denote the departure phase angle. A phase angle of zero occurs on the Earth-side of L1 and is light green in color. The value of the angle increases counter-clockwise.**

A minimum ΔV and corresponding time of flight as a function of the departure location can be stored from every arc on the discretized baseline orbit. The minimum ΔV solution for each arc as a function of departure angle and time-of-flight is shown in Figure 11. For a 20 cm/s departure maneuver, the time of flight to reach the minimum ΔV solution is approximately 370-400 days. Waiting for the minimum ΔV solution decreases the required ΔV to very manageable ranges between 6 and 12 m/s, depending on the location of the departure maneuver.

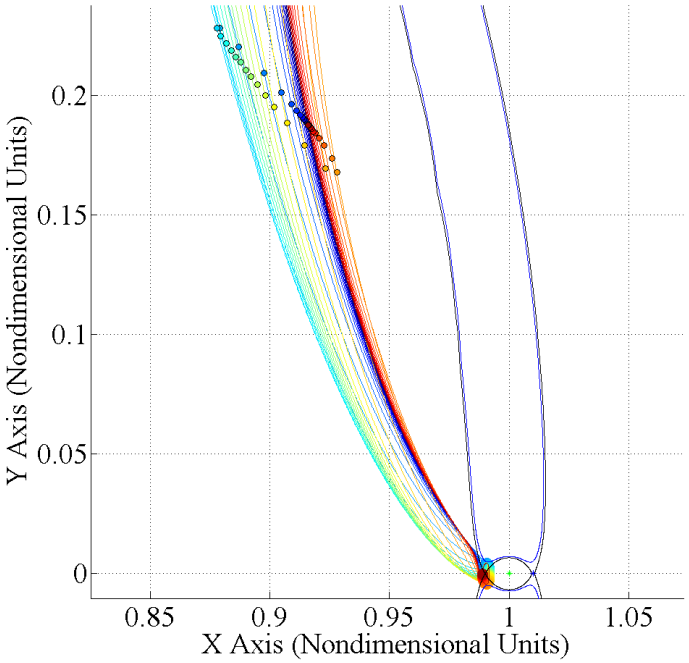


**Figure 9. Departure arcs associated with SOHO. The color scheme matches Figure 8. The black circles represent the minimum ΔV and maximum RLP velocity locations on each departure arc.**

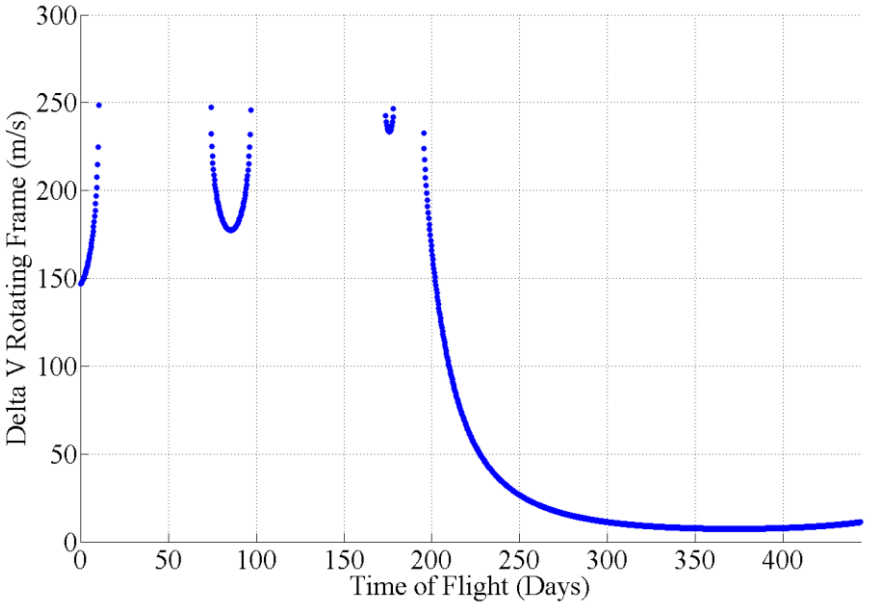


**Figure 10. ΔV along a single departure arc as a function of time of flight. The minimum solution occurs at maximum velocity locations and is between 6-10 m/s. The empty areas in the figure occur when the spacecraft is located in the zone of exclusion when trying to calculate the ΔV required to close the L1 gateway.**

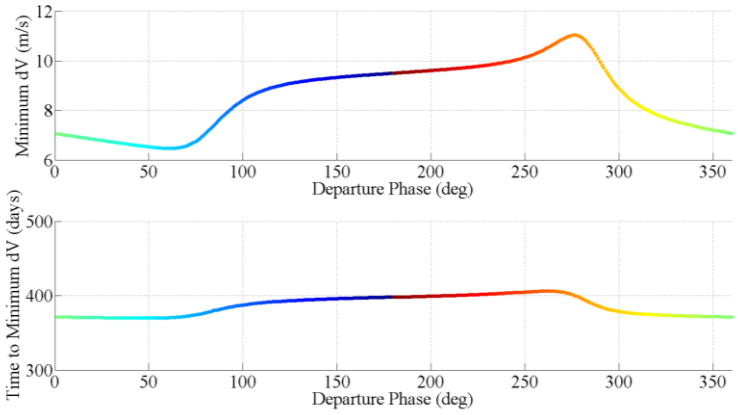


**Figure 11. The minimum ΔV solution and cooresponding time of flight as a function of the departure phase for SOHO The minimum ΔV solution is between 6 and 12 m/s with a corresponding time of flight between 370 and 400 days.**

Figure 12 contains two subplots for a single trajectory arc: the top subplot is the rotating velocity magnitude as a function of time of flight and bottom subplot is a repeat of Figure 10 with a shift in y-axis values to zoom in on the minimum ΔV solution. As seen in the figure, the minimum ΔV required to close the L1 gateway occurs when the RLP velocity magnitude reaches its maximum value. This result is in line with previous research in which the investigation found that the optimal ΔV savings location for maneuvers occurs at locations of local maximum RLP velocity.[11]

The minimum ΔV solutions are visible along the departure arcs and denoted by the circles in Figure 9. The minimum and maximum distance from the Earth-Moon barycenter to the location on the manifold is roughly 27 million and 38 million km, respectively, with an average distance of 32.7 million km. While the minimum ΔV amount may be manageable at around 10 m/s, the distance at which the minimum value occurs may present a spacecraft communications issue.

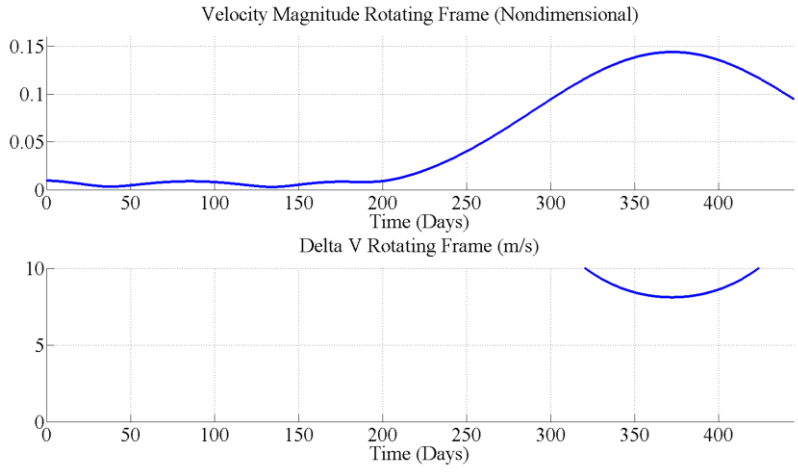


**Figure 12. The RLP velocity magnitude and ΔV required to close the L1 gateway as a function of time of flight for SOHO. The bottom subplot is a zoomed in view of Figure 10. The minimum ΔV solution occurs at the location of maximum RLP velocity.**

Similar results can be obtained for both ACE and WIND. The main difference between the spacecraft is the difference in baseline reference orbit used in the analysis. For WIND, a planar Lyapunov with appropriate RLP y and z magnitudes was selected as the baseline orbit. At a certain phase in the lifetime of the WIND mission, the Lissajous will collapse into nearly a planar Lyapunov orbit for a single revolution. Given that the energy level remains constant through the lifetime of the mission, using a planar Lyapunov orbit as the baseline is a simple way in the CR3BP model to assess the energy requirements necessary to close the L1 gateway. ACE, however, requires a little more complexity to set up since it is a small amplitude Lissajous. A multi-year propagation in a full ephemeris model using a baseline orbit determination (OD) solution was nondimensionalized and used as an initial guess for a differential corrector to create a representative orbit in the CR3BP. The result of this differential correction process can be seen visually in Figure 1.

Figure 13 shows the results for WIND and Figure 14 shows the results for ACE. Both results use the same technique of solving equation 3at each step along the departure arc and then finding the resulting minimum ΔV value for each arc. Just like SOHO, the minimum ΔV solutions for ACE and WIND L1 gateway closing maneuvers occurs at locations of local maximum RLP velocity. The ΔV value for WIND is approximately the same range as SOHO, between 5 and 10 m/s after approximately 400 days past the 20 cm/s departure maneuver, roughly in the same location between 27 million and 38 million km from the Earth-Moon barycenter. The minimum ΔV solution for ACE, however, is much lower, around 1-2 m/s and still roughly the same distance away, between 30 million and 36 million km. The similarity for SOHO and WIND is not surprising, given the similarity in the Jacobi constant for the two orbits. The Jacobi constant for the representative orbits of SOHO and WIND in the CR3BP model is 3.0008259 and 3.0008321, respectively. The Jacobi constant for ACE, however, is 3.0008836, which is much closer to the Jacobi constant for L1 of 3.0008979. The lower L1 gateway closing maneuver size for ACE makes sense given the similar energy levels between ACE and L1 and the disparity between ACE and SOHO or WIND.

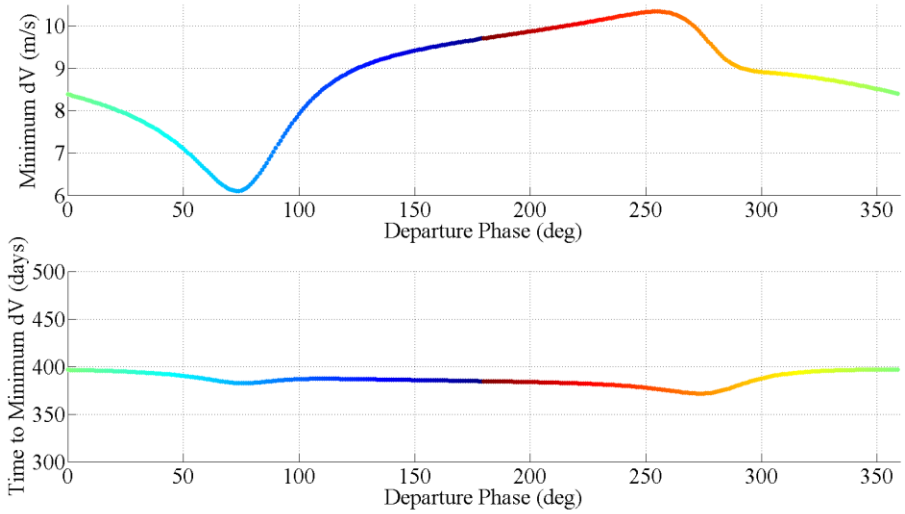


**Figure 13. The minimum ΔV solution and cooresponding time of flight as a function of the departure phase for WIND. The results for WIND are similar to SOHO as the reference orbits in the CR3BP model are very similar. The minimum ΔV solution is between 6 and 12 m/s with a corresponding time of flight between 370 and 400 days.**

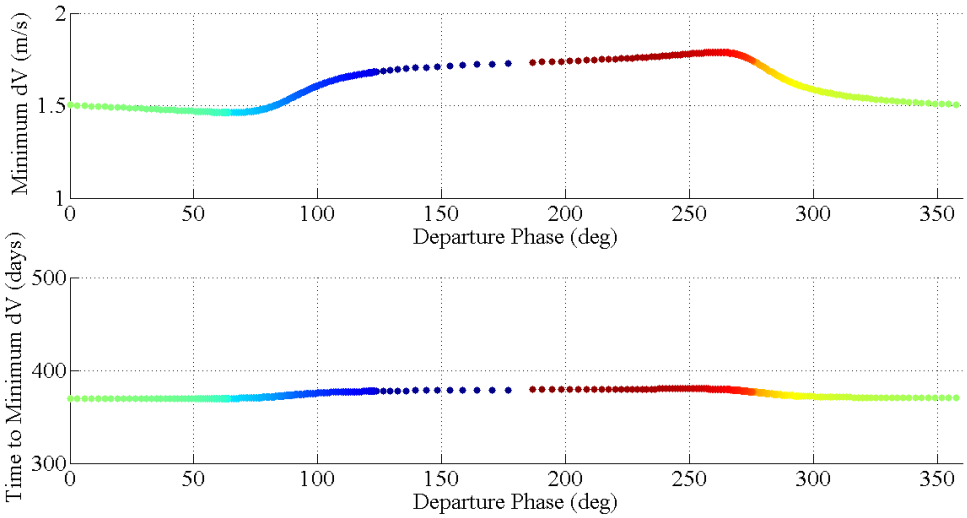


**Figure 14. The minimum ΔV solution and corresponding time of flight as a function of the departure phase for ACE. The ΔV required for ACE is much lower than WIND and SOHO between 1 and 2 m/s. The lower amount occurs because the Jacobi constant of the CR3BP reference orbit is closer to the L1 value. The time of flight, however, remains roughly the same.**

Based on the CR3BP model, reasonable ΔV values to close the L1 gateway for ACE, SOHO, and WIND are possible given enough time between the departure maneuver and the closing maneuver. Ideally, the closing maneuver will occur at local RLP velocity maximums, however waiting for over a year between the departure maneuver and closing maneuver can pose its own set of problems as the cost of sustaining operations, even at reduced staffing levels, may not be affordable if there are no additional scientific objectives to be achieved during the coast phase.

## FULL EPHEMERIS MODEL

While the CR3BP model is a helpful tool for studying the dynamics of libration point orbits, it is incapable of mimicking the effects of real world perturbations over the lifetime of a mission. For such a sensitive dynamic region, additional gravitation bodies, such as the Moon and Jupiter, can cause perturbations to the orbit over the lifetime. Another significant perturbation is solar radiation pressure. In addition, the concept of the Jacobi constant and ZVCs in a full ephemeris model become a nebulous concept due to the eccentricity of the smaller primary around the larger primary along with the addition of numerous perturbations acting on the spacecraft. While the spacecraft trajectory will be bound by an imaginary zero velocity surface, this surface will pulsate over time due to the above mentioned perturbations. Closing the L1 gateway becomes more complicated than performing a simple closing maneuver. The perturbations can have a significant effect on the orbit such that the spacecraft can return to the Earth-Moon system even with a L1 gateway closing maneuver similar to the size outlined in the CR3BP model.

To create a robust decommissioning strategy, the plan used to ensure L1 gateway closure in the CR3BP model needs to be modified to handle the consequences of unpredictable perturbations acting on the spacecraft over the course of decades. A Monte Carlo analysis is a common technique used to generate a set of statistics to analyze a given scenario involving stochastic processes. FreeFlyer was used in this investigation to provide the high fidelity dynamics.

The setup for the full force model investigation is as follows. Using an OD solution from the FDF, an operational orbit using an energy balancing station keeping technique is generated in FreeFlyer. A departure maneuver off of the operational orbit is performed at a given epoch. The spacecraft is propagated until it reaches maximum RLP velocity. As discovered in the CR3BP model, this location was found to be the location of minimum ΔV required to close the L1 gateway. Because the notion of ZVCs and a Jacobi constant is a nebulous term in a full ephemeris model, various L1 gateway closing maneuver sizes are performed. Two hundred data points exist for a given operational orbit departure date and a specific L1 gateway closing maneuver. Seven departure dates were selected, starting in January 2016 and increment in three month steps until April 2017. Each of these 200 data points are propagated for 200 years. This results in 1400 simulations for each ΔV value. Figure 15 shows one such example of a 200 year propagation in the RLP frame centered about the Sun-Earth/Moon barycenter for SOHO. For each spacecraft in the data set, the effect of SRP was varied as well. After decommissioning, the SRP area and radiation pressure coefficient will vary much more than is seen in operations, and there may be small uncertainty in the mass as well. Rather than varying each parameter separately, a ballistics-like coefficient, shown in equation 4, is randomly varied at the start of each individual sample to model the uncertain physical characteristics of the spacecraft over the duration of the 200 years.

$$\beta = \frac{Mass}{C_r \cdot Area_{SRP}} \tag{4}$$

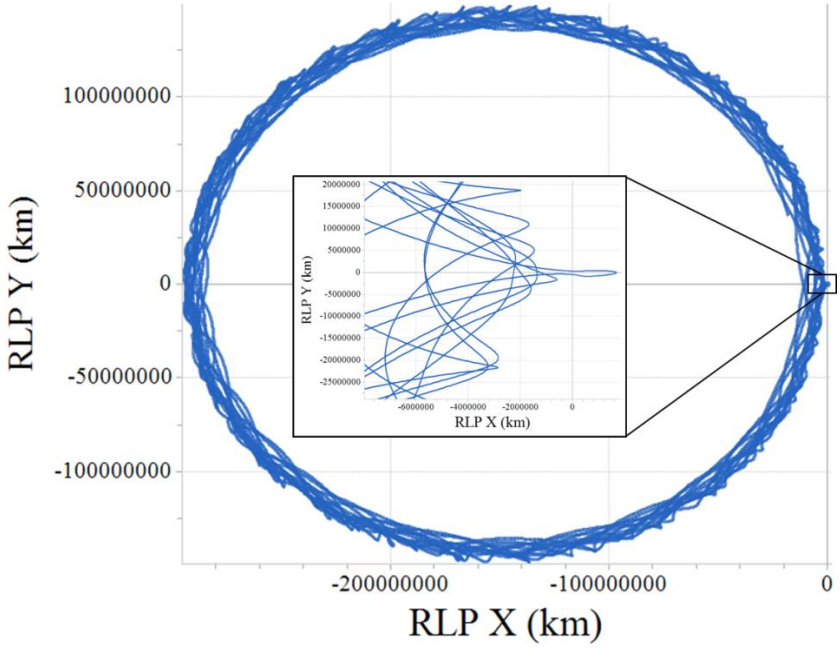


**Figure 15. A sample of a 200 year lifetime propagation for SOHO using a full ephemeris and force model. The origin is centered on the Sun-Earth/Moon L1 point.**

Once the data set has been generated, two important statistics are generated. First, the average close approach distance with respect to the Earth-Moon barycenter over the 200 year span is calculated and binned according to the size of the L1 gateway closing maneuver. In addition, the number of propagations that result in the spacecraft entering the Earth-Moon system is captured. To be more specific, entry into the Earth-Moon system is defined as the close approach distance

below 1.5 million km, or roughly the distance from the Earth-Moon barycenter to L1. An example of this close approach can be seen in Figure 15, which is a zoomed in view of Figure 15 around the Sun-Earth/Moon L1 point.

The left plot in Figure 16 visualizes the average close approach distance as a function of the L1 gateway closing maneuver for SOHO. The green line denotes the distance from the Earth-Moon barycenter to L1, 1.5 million km. The red line is a linear curve fit of the data points. The main observation from this plot is slope of the linear trend line. As the L1 gateway maneuver closing size increase, the average close approach distance increases. In a sense, the L1 gateway is shrinking in size such that the ZVCs are preventing the spacecraft from close approaches. While close approaches still happen, the general trend of increasing the close approach distance as a function of increased ΔV magnitude is apparent.

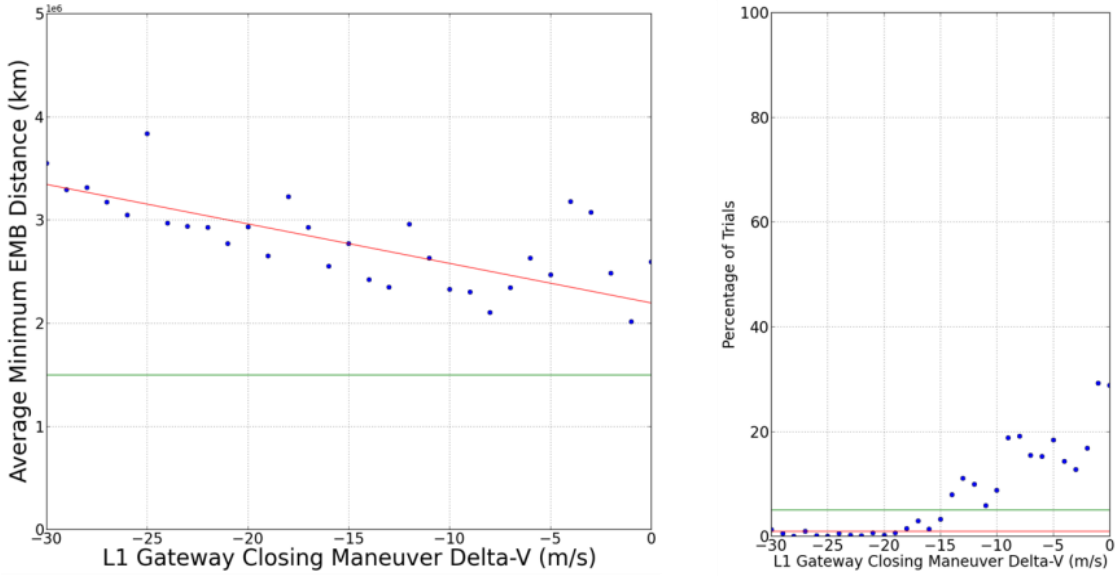


**Figure 16. Left - The average close approach distance with respect to the Earth/Moon barycenter as a function of L1 gateway closing maneuver size for SOHO. The red line is a linear curve fit. The green line is the L1 distance with respect to the Earth/Moon barycenter. Right – Percentage of trials per ΔV magnitude that re-enter the Earth/Moon system for SOHO. The green line and red line mark 5% and 1% percent respectively. The percentage drops below five percent around 15 m/s.**

The right plot in Figure 16 shows the percentage of trials that contain a close approach below 1.5 million km for a given L1 gateway maneuver closing ΔV for SOHO. The green and red line mark five and one percent thresholds, respectively. Figure 16 shows that close approaches of less than 1.5 million km are not completely eliminated for any maneuver size between 0 and 30 m/s. Based on the CR3BP model, the ΔV required to close the L1 gateway is sufficient beyond roughly 12 m/s, however, due to the perturbations associated with a full force model the larger maneuver size does not guarantee that the spacecraft will not reenter the Earth-Moon system. Once the maneuver size reaches approximately 15 m/s, the likely hood that the spacecraft will return to the Earth-Moon system after 200 years decreases below five percent. Beyond closing maneuvers of 15 m/s, the percentage drops well below five percent and below one percent for all but a handful of cases.

Similar analysis was performed for WIND and ACE, shown in Figure 17-Figure 18**Error! Reference source not found.**. For WIND, the full ephemeris model produced results very similar

to SOHO. The decrease below five percent occurs around 13 m/s, which roughly matches the CR3BP analysis. ACE also matches its CR3BP study but the decrease below five percent occurs much sooner compared to SOHO and WIND, around 6 m/s. This also matches the same result found in the CR3BP analysis where ACE requires less overall ΔV to close the L1 gateway due to the larger Jacobi constant.

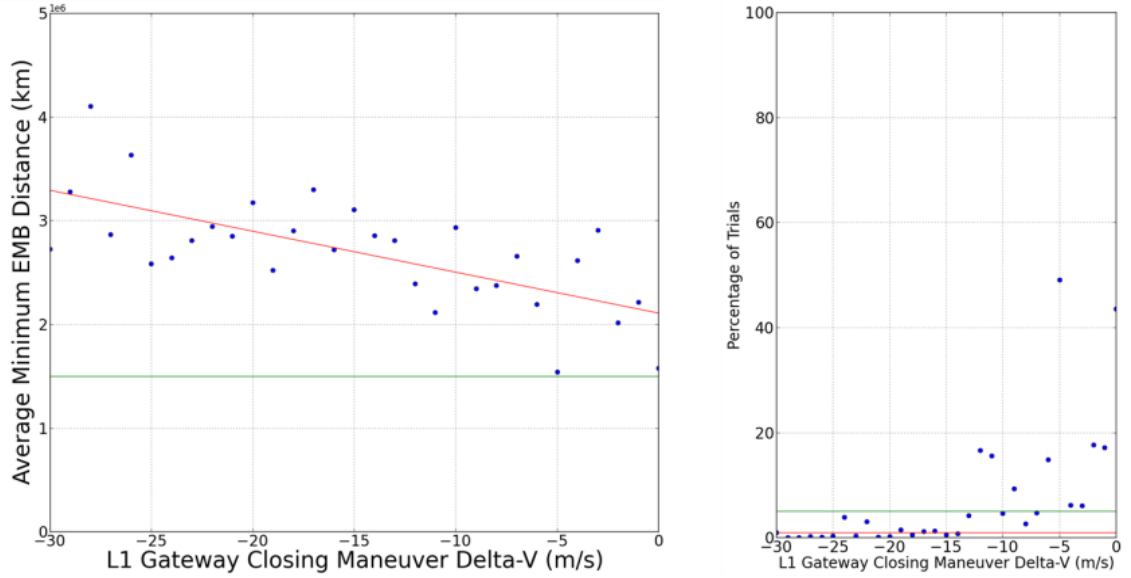


**Figure 17. Left -The average close approach distance with respect to the Earth/Moon barycenter as a function of L1 gateway closing maneuver size for WIND. Right – Percentage of trials per ΔV magnitude that re-enter the Earth/Moon system for WIND. The percentage drops below five percent around 13 m/s.**

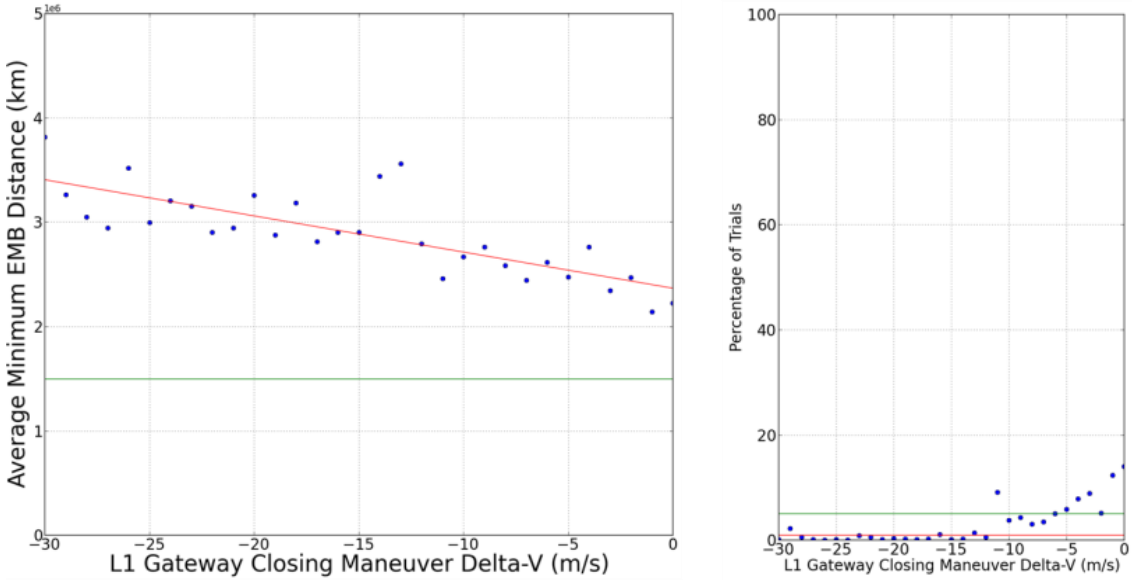


**Figure 18. Left -The average close approach distance with respect to the Earth/Moon barycenter as a function of L1 gateway closing maneuver size for ACE. Right – Percentage**

**of trials per ΔV magnitude that re-enter the Earth/Moon system for ACE. The percentage drops below five percent around 6 m/s.**

## IMPACT OF SRP MODELING AND DEPARTURE DATA

In addition to studying the ΔV closing maneuver strategy, relevant data was captured regarding the effects of the departure maneuver date along with the effect of SRP modeling. For the SRP modeling, there was no discernable pattern in the resulting close approach distance as a function of the reflectivity coefficient. Figure 19 shows the close approach distance as a function of the reflectivity coefficient used in the spacecraft model within FreeFlyer. The plot contains all 1400 data points for a given ΔV closing maneuver of 23 m/s for SOHO. For a given ballistics coefficient, there is no pattern for the close approach distance. Long term propagation imparts enough of a perturbation such that the ballistics coefficient used has no effect on the close approach distance.

While there may be no pattern between the ballistic coefficient and the resulting close approach distance, the appearance of horizontal lines in Figure 19 indicates a kind of repeatable close approach distance. Figure 20 visualizes the resulting close approach distance for all 1400 cases from the 23 m/s closing maneuver for SOHO. Each departure epoch is binned into increments of 200. As an example, a departure date of January 2016 occurs between points 0-199, April 2016 occurs between 200 and 399, and so on. During the January 2016 simulation (bin 0-199), there is a remarkably consistent close approach distance. This result was unexpected and could warrant future study to determine if there is any scenario in which this tight close approach distance can become predictable. As of right now, there is no explanation available for this behavior but could become a topic of future investigation to determine if there a way to leverage this behavior for decommissioning strategies.

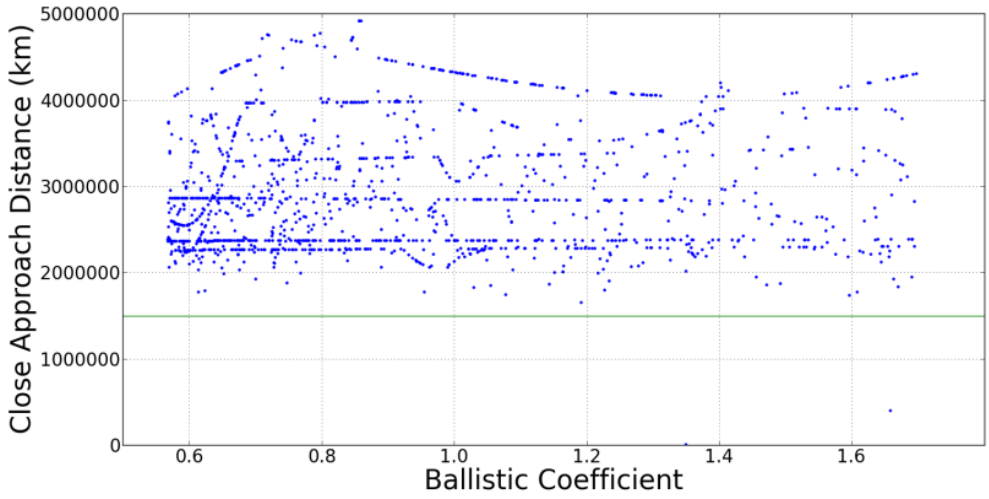


**Figure 19. The close approach distance as a function of the ballstic coefficient for a ΔV of 23 m/s. There is no discernable pattern between the ballistic coefficent and the close approach distance.**

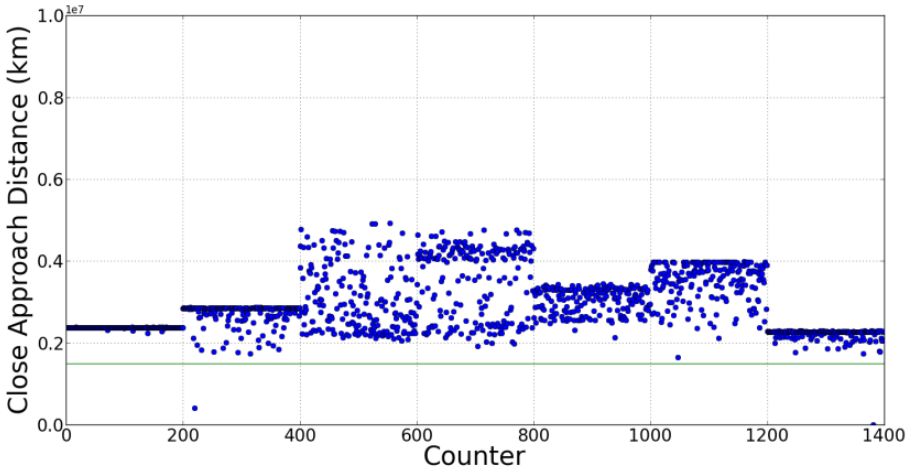


**Figure 20. The resulting close appraoch distance for each trial run for a ΔV of 23 m/s. The points are binned in groups of 200 based on the departure date. A tight grouping exists, regardless of ballistic coefficient. One such example occurs for the 0-199 bin.**

## OPERATIONAL CHALLENGES

Each of the three missions presents unique challenges for implementing this strategy operationally. For SOHO, as mentioned before, the thruster duty cycle is limited to 5%. For a maneuver on the order of 15 m/s, the duration would exceed a single view period with the DSN and would likely need to be divided across several days. Also, the attitude would need to be changed from pointing the instrument toward the Sun and instead point the high gain antenna toward the Earth. This would preclude any scientific observations during the period between the L1 departure maneuver and the second, larger decommissioning burn.

WIND has a history of performing several large maneuvers using different thruster combination prior to reaching the current libration point orbit in 2004; thus it would likely present the fewest challenges operationally. ACE also has a history of performing very large maneuvers with all thrusters, but like SOHO, it would require a different attitude control strategy in order to keep the antenna pointing toward Earth during the transfer period from the operational orbit to the decommissioning location. In addition, ACE has the lowest amount of fuel remaining out of the three missions. Although its orbit requires the smallest change in Jacobi constant to close the L1 gateway, all of the propellant may be consumed maintaining the current orbit and attitude.

One final challenge, related to all three missions, is the staffing level during the cruise and L1 gateway closing maneuver. Given that the time of flight is upwards of a year, the mission would require funds to maintain the operations staff. As this current time, discussions on staffing and funding levels have not occurred and would need to occur if this strategy were to be implemented in the future. Additional analysis into balancing the time of flight and location of the L1 gateway closing maneuver may be necessary if funding levels are an issue. The spacecraft have sufficient fuel such that the maneuver does not need to be performed at the most efficient location.

## CONCLUSION

This investigation demonstrated the feasibility in closing the L1 gateway as a decommissioning strategy for ACE, WIND, and SOHO. First, a CR3BP approximation was used to determine the ΔV costs associated with closing the L1 gateway. Minimum ΔV values were found ranging from 6-12 m/s for SOHO and WIND and 1-2 m/s for ACE when performing the L1 gateway clos-

ing maneuver at the location of maximum RLP velocity. The analysis was extended into a full ephemeris model and a Monte Carlo simulation was performed to model the perturbations applied by other celestial bodies and the effects of SRP acting on the spacecraft over a 200 year span. The results from the Monte Carlo roughly agreed with the ΔV ranges found from the CR3BP study. The percentage of cases returning to the Earth-Moon system decreases below five percent at 15 m/s for SOHO, 13 m/s for WIND and 6 m/s for ACE.

Future investigations could study the effect of the departure phase in the full ephemeris model, especially when a realistic date for decommissioning each spacecraft is more certain. In addition, future work could try to explain the consistent minimum Earth/Moon barycenter distance phenomenon found in the SRP analysis section. Finally, discussion needs to occur with each project to determine what modifications need to be made to the decommissioning strategy proposed in this study in order to accommodate real world operational constraints and limitations.

## ACKNOWLEDGMENTS

This work was conducted under NASA contract # NNG14VC09C.

## REFERENCES

[1] E. Alessi, C. Colombo, M. Landgraf, "Re-entry Disposal Analysis for Libration Point Orbit Missions," *24th International Symposium on Space Flight Dynamics*, 5-9 May 2014, Laurel, Maryland.

[2] M. Schmidt, F. Keck, "The End of Life Operations of the Herschel Space Telescope," *SpaceOps Conference*, 5-9 May 2014, Pasadena, CA.

[3] Z. Olikara, G. Gomez, and J. Masdemont, "End-Of-Life- Disposal of Libration Point Orbit Spacecraft," *64th International Astronautical* Congress, 2013, Beijing, China..

[4] C. Roberts, "Long Term Missions at the Sun-Earth Libration Point L1: ACE, SOHO, and WIND," *AAS/AIAA Astrodynamics Specialist Conference*, 31 Jul. – 4 Aug. 2011, Girdwood, Alaska.

[5] C. Roberts, "The SOHO Mission L1 Halo Orbit Recovery from the Attitude Control Anomalies of 1998," *Libration Point Orbits and Applications Conference*, 10-14 Jun. 2002, Girona, Spain.

[6] J. Brown and J. Petersen, "Applying Dynamical Systems Theory to Optimize Libration Point Orbit Stationkeeping Maneuver for WIND," *AIAA/AAS Astrodynamics Specialist Conference*, 4-7 Aug. 2014, San Diego, California.

[7] H. Franz, P. Sharer, K. Ogilvie, and M. Desch, "WIND Nominal Mission Performance and Extended Mission Design," *The Journal of the Astronautical Sciences*, Vol. 49, No. 1, January-March 2001, pp. 145-167.

[8] H. Franz, "WIND Lunar Backflip and Distant Prograde Orbit Implementation," *AAS/AIAA Space Flight Mechanics Meeting*, 11-15 Feb. 2001, Santa Barbara, California.

[9] H. Franz, "Design of Earth Return Orbits for the WIND Mission," *AAS/AIAA Space Flight Mechanics Meeting*, 27-30 Jan. 2002, San Antonio, Texas.

[10] H. Franz, "A WIND Trajectory Design Incorporating Multiple Transfers Between Libration Points," *AIAA/AAS Astrodynamics Specialist Conference*, 5-8 Aug. 2002, Monterey, California.

[11] T. Sweetser, "Jacobi's Integral and ΔV-Earth-Gravity-Assist (ΔV-EGA) Trajectories," AAS 93-635.